ELSEVIER

Thermochimica Acta 381 (2002) 139–146

thermochimica acta

www.elsevier.com/locate/tca

The use of infra-red light-modulated temperature in DSC created by pulse-width modulation

P. Kamasa[a,b], A. Buzin[a,b], M. Pyda[a,b], B. Wunderlich[a,b,*]

[a]*Department of Chemistry, The University of Tennessee, Knoxville, TN 37996-1600, USA*
[b]*Chemical and Analytical Sciences Division, Oak Ridge, National Laboratory, Oak Ridge, TN 37831-6197, USA*

Received 7 March 2001; accepted 2 June 2001

Abstract

Infra-red light, generated by diodes, is applied to produce a sinusoidal temperature modulation in the standard heat-flux DSC of TA instruments. The temperature of the sample and reference are controlled by both, the original temperature controller of the instrument, and by the radiant energy generated by two high-power infra-red light-emitting diodes (LEDs). This allows for isothermal or quasi-isothermal experimentation in the standard mode of operation of the calorimeter. The additional infra-red irradiation is provided only for temperature modulation. The radiant energy transferred to the specimens is controlled by pulse-width modulation (PWM) which provides a high linearity in the temperature modulation program. This feature enables to obtain any arbitrary temperature profile with the limits of frequency set by the calorimeter response and speed of the computer. Simple electronics and a computer algorithm for the PWM control are described. The method was tested in the melting range of indium and by measurement of the heat capacity of sapphire (Al_2O_3) and polystyrene. The problem of frequency correction arising from a wide frequency range is analyzed and discussed. Published by Elsevier Science B.V.

Keywords: Temperature-modulated DSC; Infra-red-modulated temperature; Pulse-width modulation

1. Introduction

Temperature-modulated differential scanning calorimetry (TMDSC) had its beginning in 1992 with the introduction of the first commercial calorimeter by TA instruments, Inc. [1]. The special features of the TMDSC—an evaluation of the thermal effects as a response to the temperature modulation—has become an established tool in thermal analysis. The TMDSC had found wide application in the study of melting and crystallization of polymers as well as the glass transition and other irreversible phenomena. Since the introduction of TMDSC many specia techniques have been developed, including multifrequency modulation accomplished with a complex sawtooth [2]. This technique was applied to a detailed calibration of all three of the common commercial DSC equipment from TA instruments [3], Mettler–Toledo [4], and Perkin-Elmer [5]. Identical measurements were attempted with a step-isotherm modulation generating a multifrequency temperature profile using the Perkin-Elmer Pyris-1 DSC [6]. In all these experiments the commercial calorimeters were not modified, running in the standard mode of temperature control.

* Corresponding author. Tel.: +1-675-974-0652; fax: +1-675-974-3454.
E-mail address: athas@utk.edu (B. Wunderlich).

0040-6031/02/$ – see front matter. Published by Elsevier Science B.V.
PII: S0040-6031(01)00649-9

Besides conventional heaters, radiant energy as a heating source has been used to modulate temperature in ac calorimetry. A tungsten lamp, for instance, and a mechanical chopper were used to provide periodic heating. Carrington et al. [7] has constructed an ac differential calorimeter, which used light-emitting diodes (LEDs). A calorimeter with a laser diode as a heating source was used by Marone and Payne [8] in a study of phase transitions of semiconductors. In case of diodes, the radiant energy is modulated electronically, usually by a square wave derived from a lock-in amplifier, providing better frequency lock-in comparison to a mechanical chopper. The main disadvantage of squarewave modulation is an uncontrolled content of higher harmonics in the temperature-modulated profile. A sinusoidal temperature profile was obtained by Saruyama [9] where the intensity of the light was modulated with two polarizers, one rotated by a stepping motor and the other one fixed. The method allows to obtain a purely sinusoidal temperature profile over a wide frequency range, but it was limited to a single frequency measurement. In this paper the TMDSC obtained by infra-red light as an additional heating source (LMDSC) is described. The experimental set allows programming using a sinusoidal as well as a multifrequency temperature profile.

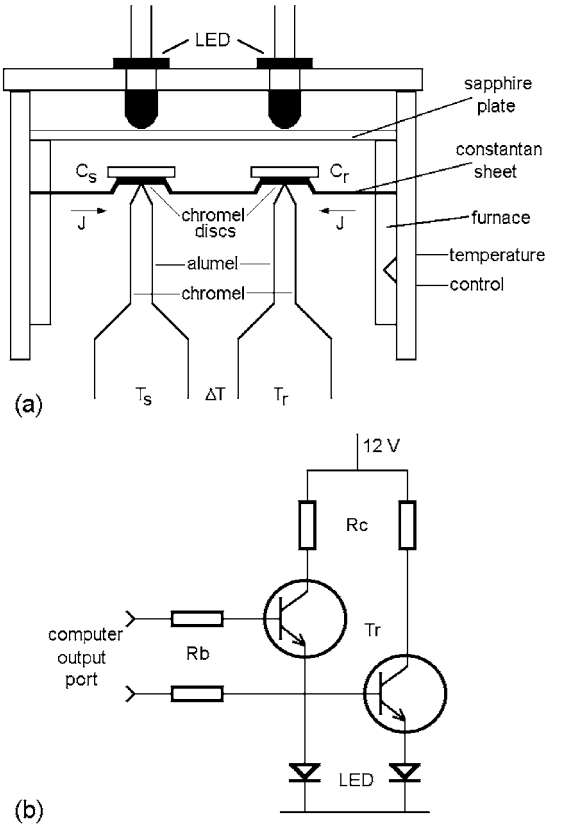

Fig. 1. Position of the infra-red LEDs in the measuring cell and electrical scheme for the driving current.

2. Experimental

The LMDSC method was procured by modifying a commercial DSC of the heat-flux type, a TA instruments 2910 DSC, operated in the standard mode with air cooling. The experimental arrangement is shown in Fig. 1a, the electronics is outlined in Fig. 1b. Two high-power LEDs are placed in the cover of the DSC cell as indicated in Fig. 1a. Each of the LEDs had a radiant power output of 100 mW at 100 mA of current (Radio Shack Cat. #276-143c). The radiant energy from a distance of 4 mm is focused on the top of the sample and reference aluminum pans. The surfaces of the covering lids were optionally sprayed with an ultra-flat black paint for more efficient light absorption. For higher temperatures, graphite-based blackening is possible, but measurements were also successful without modification of the aluminum pans. The temperature for the isothermal or quasi-isothermal modulation profile is controlled and stabilized by the temperature controller of TA instruments, operating in the standard mode. A single sapphire disc covered the measuring cell to avoid unnecessary heat losses to the environment and to protect the LEDs from overheating. The sapphire disc is transparent in the 0.3–0.4 μm infra-red region, and drops to about 60% transmittance by 5 μm which corresponds to the wavelength of the emitted light. The current through the LEDs is controlled by transistor-emitter followers, Tr, as shown in Fig. 1b. The LEDs are operating at saturating current, limited by the resistors Rc. Under this condition the intensity of the light depends only slightly on temperature and only a small instability results from the current itself. The transistors are operating in the switching mode and can be driven from any I/O computer port, in our experiment the printer port. This scheme allows obtaining temperature control by changing the pulse-width, the method known as

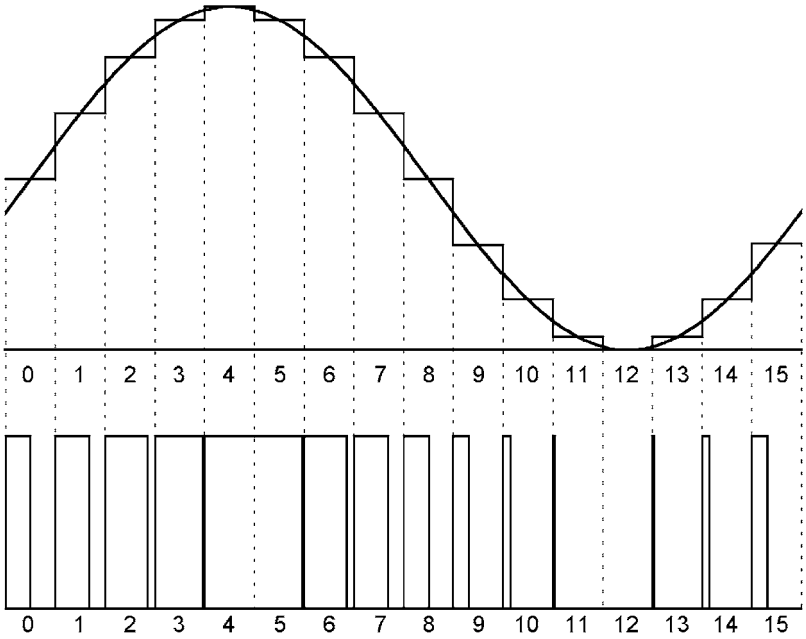

Fig. 2. Principle of the PWM method. The width of the pulses in the lower trace is proportional to the value of the sine-function shown in the upper trace. The basic time intervals are labeled as $n = 0$–15.

a pulse-width modulation (PWM) and was developed in the field of information transmission.

The computer program developed generates a series of pulses as illustrated in Fig. 2. Time is divided into n equal intervals of 0.125 s as a basic unit. These intervals are subdivided into 128 divisions, each of which is separately programmed to one from two possible states, high or low. The high and low state corresponds to the emission or dark state of the diodes, respectively. The duration of the light emission over one basic interval is proportional to the instantaneous value of the modulation function. Due to the large heat capacity of the calorimeter, the temperature has a mean value proportional to the power emitted during the large number of basic intervals. As an example, a sinusoidal program and corresponding temperature response are illustrated in Fig. 3. A digitally generated table is displayed in the upper window. The period of 243 s contains 1944 discrete values ($1944 \times 0.125\,\text{s} = 243$ s). When running the program, the temperature is changing sinusoidally. The measured temperature and corresponding heat-flow for 22 mg of sapphire are illustrated in the lower window of Fig. 3. The temperature profile was analyzed using a Fourier-transform and

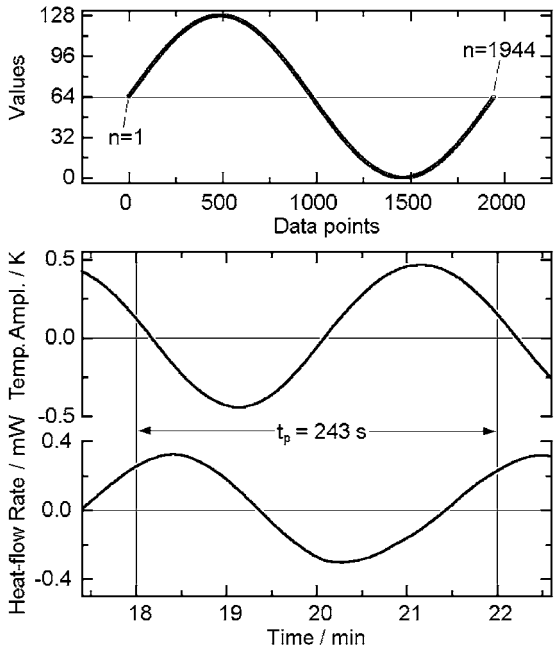

Fig. 3. Sample temperature and heat-flow obtained by PWM according to the program shown in the upper window.

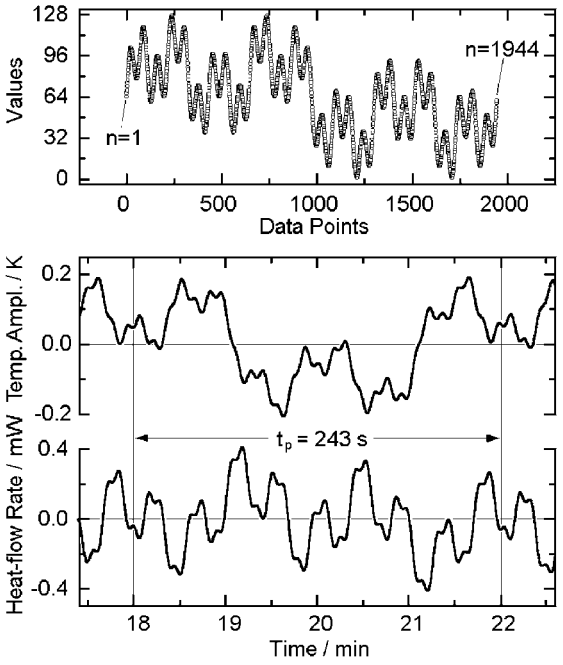

Fig. 4. Multifrequency program consisting of four sinusoidal components of the periods: 243, 81, 27, 9 s. The temperature response and corresponding heat-flow rate are displayed in the lower window.

has a negligible content of higher harmonics and was measured to be $<10^{-4}$.

A multifrequency program is illustrated in Fig. 4. The upper trace shows the digitally generated waveform, consisting of four harmonics with periods of 243, 81, 27, and 9 s, each sequentially lower period being the third harmonic of the former. Such choice seems to be optimal to obtain a wide frequency range covering 27 harmonics with a minimum of unavoidable losses due to amplitudes shared between the different harmonics.

3. Testing and results

The new method was next tested using such standard substances as indium, sapphire, and polystyrene. Single and multifrequency temperature profiles were applied. The aim of the test with indium was to check the effectiveness of temperature modulation using LEDs. The frequencies chosen for the measurement of the temperature–frequency responses had periods of 243, 100, 81, 50, 27, 9, and 3 s. The experiment was carried out in the standard mode of the calorimeter with an underlying heating rate of 0.2 K min^{-1}. The raw data of the sample temperature and the heat-flow rate at a single frequency of 1/27 Hz are illustrated in Fig. 5a. In the region of melting one can see a different slope of the underlying heating rate which recovers only after melting is complete, a characteristic for the standard DSC [10,11]. The observed decrease in amplitude of modulated temperature together with the increasing amplitude of the heat-flow rate indicates that parts of the sample are modulated, while other parts are melting. The temperature of the sample could be modulated with periods down to 9 s. On the other hand, the non-zero amplitudes during melting indicate a difference between the measured temperature and a distribution of temperatures within the sample, which during equilibrium-melting should not exist. A more detailed look at the experiment in the region of beginning of melting can be seen in Fig. 5b. It represents a magnification of region I of Fig. 5a. Below melting temperature T_m, which is seen before point A in the time scale of Fig. 5b, the temperature and corresponding heat-flow rate are governed by the heat capacity of the indium crystals. At the point A, one can detect a discontinuity in the heat-flow rate which indicates that melting has started on reaching T_m. Up to point B, melting is continued, but only a small portion of the sample, the outer layer, has melted. Earlier temperature measurements by contact-less infra-red thermography had shown that the top and bottom of the aluminum pan are almost at the same temperature [12], which means that the inner part of the sample is last to melt. At point B, the melting temperature has again been reached during the off-cycle of the LEDs and the melted outer portion starts to recrystallize. The recrystallization occurs without supercooling since crystal nuclei remain in the sample. The end of the recrystallization is observed at point C as another discontinuity in the heat-flow rate. Between points C and D all indium is crystallized again, and the heat-flow rate, as well as the temperature, are determined by the heat capacity of the crystalline indium, as it was before point A. At point D, T_m is reached and renewed melting starts. Because of the underlying heating-rate, the second melting cycle of the sample continues for a longer time. The decrease in modulation amplitude of the

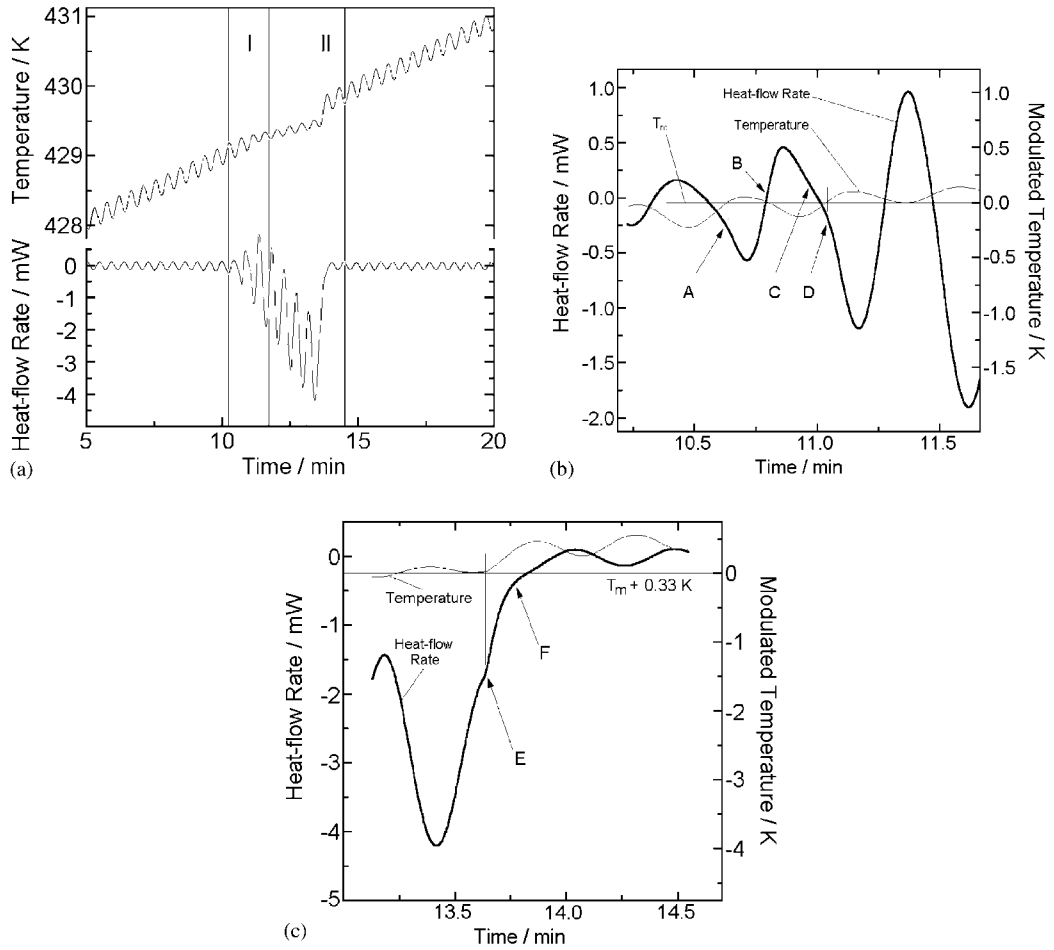

Fig. 5. Test with indium in the melting-temperature range, using an underlying heating rate of 0.2 K min^{-1} and the PWM method with a modulation period of 27 s. (a) Overall view of the experiment, the temperature scale can be calibrated by shift to the begin of melting shown in the magnification (b). (b) Magnified region I which shows melting in region A to B and beyond D, and crystallization in region B to C. The modulated temperature scale is centered about the melting temperature. (c) Magnified region II which shows melting up to E, and recovery of steady state without melting and crystallization between E and F. The modulated temperature scale is centered about the melting temperature.

temperature with the increased heat-flow can be seen best from Fig. 5a. Two facts contribute to the difference of the temperature amplitude from the expected zero value during melting. One is based on the thermal resistances between sample, pan, and thermocouple and the limited thermal conductivity of the sample. The second is that melting and crystallization processes are not necessarily instantaneous, both, the maximum heat exchanged between the sample and the calorimeter and the transition kinetics is finite. Starting from point D in Fig. 5b, melting is continuous without recrystallization. Still, the melting-rate is sinusoidally changing because of the limited melting during a single modulation cycle. The same observations were made earlier with quasi-isothermal TMDSC on heater and sample-temperature governed modulation [10,11]. In the case of indium, a sample of high thermal conductivity and with a fast melting rate [13], the amount of melting is most likely determined only by the limited delivery of heat from the calorimeter. The sample reaches a quasi-stationary state with a constant amount of melting taking place within each cycle until all indium is melted. This final stage of melting is observed in region II of Fig. 5a, magnified

in Fig. 5c. The melting process is complete at point E. At about point F, the amplitude of the heat-flow rate and temperature are again determined by the heat capacity of the indium, but now in the liquid state.

In other experiments it was found, that the temperature of the sample was modulated with periods as small as 9 s. All lags within the calorimeter mentioned above are frequency dependent, and therefore, for the calculation of heat capacity, appropriate corrections can be done. Using a model of the heat-conduction path between the temperature sensor and the pan, and then the pan and the sample, the correction of the heat capacity determination in a temperature-modulated DSC was considered in detail [14,15]. The apparent heat capacity is in this case calculated from the amplitude of the modulated temperature of the sample, A_{T_s}, and amplitude of heat-flow rate A_Φ:

$$C_p^{\#} = \frac{A_\Phi}{A_{T_s}\omega} K(\omega) \tag{1}$$

where ω is the angular frequency and $K(\omega)$ is an empirical correction function: $[1 + (\tau\omega)^2]^{1/2}$. The correction becomes insufficient when higher frequencies are applied and not only because a radiant source is used as a heater. This problem is discussed next, based on more general assumptions.

The amplitudes of the modulated temperature and the heat-flow rate response were measured as a function of frequency. As is indicated in Fig. 6, the measured amplitudes of the modulated temperature decrease with frequency, determining the frequency range of use. One can distinguish three regions. First, in the low-frequency range there is only little frequency-dependence of the amplitude. If the frequency is low enough, the sample temperature follows the temperature program and is equal to the dc measurement. In the second region, in the middle-frequency range, the amplitude strongly decreases. Finally, in the third, high-frequency region, the temperature is not modulated anymore. This behavior is common for all of linear systems for which the response to small perturbations (temperature) may be described by the differential equation:

$$\frac{dT}{dt} = -\frac{1}{\tau}(T - T_0) \tag{2}$$

where T_0 is a final temperature, and τ represents a time constant characterizing how the system returns to the

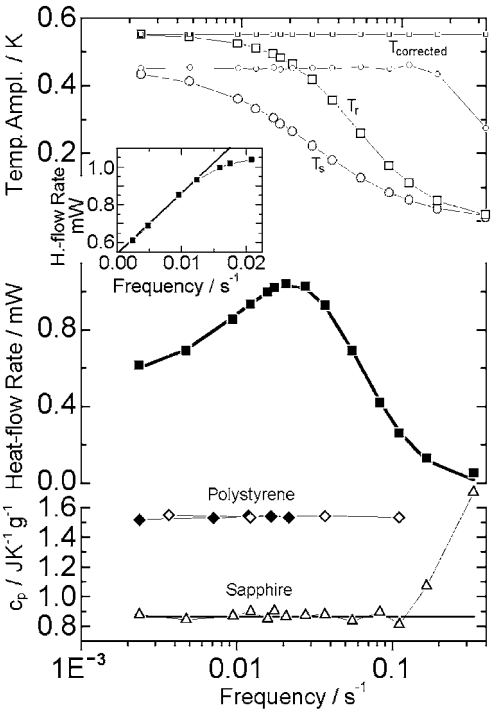

Fig. 6. Measured and corrected sample and reference temperatures at 369.5 K (○, ∘ and □, □, respectively), the corresponding heat-flow rates (■) and specific heat capacities of sapphire (Al_2O_3) and polystyrene.

equilibrium. The solution of the Eq. (2) transformed to the frequency domain $T(\nu)$ yields a complex function consisting of

$$A'_T(\nu) = T_0 + \frac{A_T}{1 + (\nu\tau)^\alpha} \quad \text{and} \quad A''_T(\nu) = \frac{(\nu\tau)^{\alpha/2} A_T}{1 + (\nu\tau)^\alpha} \tag{3}$$

where A_T is the temperature amplitude and ν is frequency in Hz. The time constant τ characterizes the thermal relaxation of the system. In real systems, the relaxation process is distributed between different paths of dissipation having no singular time constant, and the exponent α in Eq. (3) is usually different from two. It is expected that they will describe the temperature distribution in the calorimeter. In Fig. 6 the amplitude of the sample temperature measured as a function of frequency is represented by the symbols (○). The solid line is the approximated real part of Eq. (3) with a minimum of the mean square error

(MSE) obtained for $\tau_s = 36.8$ s and $\alpha_s = 1.314$ and $A_{T_s} = 0.4521$ K (index s denotes the sample). One can see good agreement with the experimental values. The amplitude of the heat-flow rate is displayed in the lower trace by the symbols (■). Down to a frequency of about 0.01 Hz (a period of 100 s) the heat-flow increases linearly (see the insert in Fig. 6, plotted linearly), and after a maximum at 0.02 Hz, it decreases monotonously to zero. In this frequency region the correction used in Eq. (1) holds.

Having the data from the whole frequency range, where sample temperature and heat-flow has measurable values, we propose further analysis and corrections to obtain the heat capacity at higher frequencies.

Due to the symmetry of the two sides of the calorimeter, the changes of the amplitude of the reference have the same character and can be approximated to the same function, however, with different parameters of A_T, τ and α. The reference temperature can be estimated from the definition of the heat-flow rate as a difference between the amplitudes of reference and sample temperature:

$$A_\Phi(\nu) = K\left(\frac{A_{T_r}}{1 + (\nu\tau_r)^{\alpha_r}} - \frac{A_{T_s}}{1 + (\nu\tau_s)^{\alpha_s}}\right) \tag{4}$$

where K is the Newton's law constant. For experimental data of the heat-flow rate A_Φ and the previously found A_{T_s}, τ_s and α_s, the parameters for the reference temperature A_{T_r}, τ_r, and α_r as well as the constant K can be found by a second approximation as $\tau_r = 19.219$ s, $\alpha_r = 1.794$, $A_{T_s} = 0.551$ K and $K = 5.259$. The constant K was also obtained from an experiment applying light modulation only to the sample side. A heat exchange between both sides was compensated by measuring the temperature at the sample position when modulation was applied only to the reference position and then K was estimated by taking the corrected sample temperature as $K = A_\Phi/(A_{T_s} - A_{T_r})$. Obtained value of K varies from 5 to 6 J s^{-1} K^{-1} for modulated period between 420 and 9 s. Taking experimental values of the sample temperature and approximated reference temperature, the heat-flow was reconstructed indicated by the solid line in Fig. 6. The reference temperature that was obtained as $A_{T_r} = (A_\Phi/K) + A_{T_s}$ is depicted in Fig. 6 by the symbols (□) and the corresponding solid line is the approximation.

From the information about temperature at the sample and reference positions, the correction to frequency-independent temperatures A'_{T_r} and A'_{T_s} is obtained by division of the experimental data by the corresponding approximations. Corrected temperatures are displayed by small symbols (○, □) in Fig. 6. In the range up to 0.1 Hz, the temperatures have constant values, and are frequency-independent. A heat capacity may be calculated for every frequency from:

$$C_p = \frac{KA'_{T_r}}{A'_{T_s}\omega} \tag{5}$$

where K is the previously obtained Newton's law constant and ω is the lowest frequency. The heat capacity corrected to the reference data of sapphire and displayed as the lower trace (Δ) of Fig. 6. The error from the mean value is ±2% at lower frequency with small increases at higher frequency. Above the frequency 0.11 Hz (period 9 s) the measurement becomes unreliable. The above correction procedure was applied also to the data gained from similar runs made to obtain the heat capacity of polystyrene in the same frequency range. The results corrected with the heat capacity of sapphire at the same temperature are illustrated in Fig. 6 by the symbols (◇). In the temperature range below the glass transition. The heat capacity of polystyrene is frequency independent and the obtained results are in good agreement with earlier results from quasi-isothermal multifrequency sawtooth modulation of standard TMDSC (◆) [6].

4. Conclusions

The temperature-modulated calorimetry has recently experienced a strong increase in interest, and new methods of modulation and analysis have been developed. The advantage of light-modulated DSC using PWM technique is the possibility to obtain multifrequency temperature programs over wide frequency ranges. On the example of the heat-flux type calorimeter it was demonstrated, that the heat capacity can be obtained for higher frequency than possible in the standard mode of operation. The heat capacity of the calorimeter rather than the electronics and the computer program determine the limiting frequency. Since the method is electronically able to cover a 10 times wider frequency range than demonstrated, the light-modulation may be applied to other types of

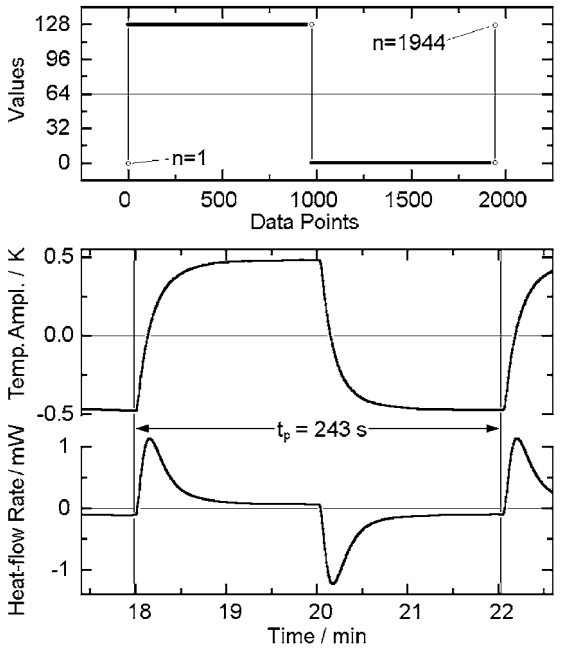

Fig. 7. Temperature modulation with a square waveform (upper window) and the corresponding temperature and heat-flow rate responses (lower window).

instruments having faster response times. The applied PWM method enables also to obtain sinusoidally or programmed temperature profile at low frequencies. When using a simple square wave, a long period compared with time constant of the calorimeter yields a steady state where the heat-flow has non-zero value only at the beginning of each period. This is illustrated in Fig. 7 where the temperature is programmed as a rectangular function of period 243 s. This type of modulation is analogous, however, to the meander type of modulation, applied and analyzed as discussed by Kamasa et al. [6]. The aim of the presented work was to prepare the experimental background for the evaluation of the kinetics of the glass transition for which it is necessary to carry out experiment over a wider frequency range than otherwise obtainable by TMDSC. Results of this application will be prepared in the near future [16].

Acknowledgements

This work was supported by the Division of Materials Research, National Science Foundation, Polymers Program, Grant # DMR-9703692 and the Division of Materials Sciences and Engineering, Office of Basic Energy Sciences, US Department of Energy at Oak Ridge National Laboratory, managed and operated by UT-Batelle, LLC, for the US Department of Energy, under contract number DOE-AC05-00OR22725. Support for instrumentation came from TA instruments, Inc.

References

[1] M. Reading, B.K. Hahn, B.S. Crowe, Method and apparatus for modulated differential analysis, US Patent 5 224 775 (1993).
[2] B. Wunderlich, R. Androsch, M. Pyda, Y.K. Kwon, Thermochim. Acta 348 (2000) 181.
[3] M. Pyda, Y.K. Kwon, B. Wunderlich, Thermochim. Acta 367/368 (2001) 217.
[4] J. Pak, B. Wunderlich, Thermochim. Acta 367/368 (2001) 229.
[5] Y.K. Kwon, R. Androsch, M. Pyda, B. Wunderlich, Thermochim. Acta 348 (2000) 181.
[6] P. Kamasa, M. Merzlyakov, M. Pyda, J. Pak, C. Schick, B. Wunderlich, Thermochim. Acta, accepted for publication.
[7] A. Carrington, A.P. Mackenzie, A. Tyler, Phys. Rev. B 54 (1996) R3788.
[8] M.J. Marone, J.E. Payne, Rev. Sci. Instrum. 68 (1997) 4516.
[9] Y. Saruyama, Thermochim. Acta 304/305 (1997) 171.
[10] A. Boller, M. Ribeiro, B. Wunderlich, in: R.J. Morgan (Ed.), Proceedings of the 25th NATAS Conference, Vol. 25, McLean, VA, 1997, p. 706.
[11] B. Wunderlich, A. Boller, I. Okazaki, K. Ishikiriyama, W. Chen, M. Pyda, J. Pak, I. Moon, R. Androsch, Thermochim. Acta 330 (1999) 21.
[12] R. Androsch, M. Pyda, H. Wang, B. Wunderlich, J. Thermal Anal. Cal. 61 (2000) 661.
[13] M. Jaffe, B. Wunderlich, in: E.F. Schwenker, P.D. Garn (Eds.), Proceedings of the 2nd ICTA on Thermal Analysis, Vol. 1, Academic Press, New York, 1969, p. 387.
[14] I. Moon, R. Androsch, B. Wunderlich, Thermochim. Acta 357/358 (2000) 285.
[15] R. Androsch, I. Moon, S. Kreitmeier, B. Wunderlich, Thermochim. Acta 357/358 (2000) 267.
[16] P. Kamasa, M. Pyda, A. Buzin, B. Wunderlich, in preparation.